European Journal of Medicinal Chemistry 90 (2015) 742–750

Contents lists available at ScienceDirect

European Journal of Medicinal Chemistry

journal homepage: http://www.elsevier.com/locate/ejmech

Original article

Novel fluoroalkyl derivatives of selective kappa opioid receptor antagonist JDTic: Design, synthesis, pharmacology and molecular modeling studies

Sébastien Schmitt [a, b, c], Nathalie Colloc'h [b, c, d], Cécile Perrio [a, b, c, *]

[a] CNRS, UMR 6301 ISTCT, LDM-TEP, GIP CYCERON, Boulevard Henri Becquerel, 14074 Caen, France
[b] Université de Caen Basse-Normandie, Normandie Univ., France
[c] CEA, DSV/I2BM, France
[d] CNRS, UMR 6301 ISTCT, CERVOxy group, GIP CYCERON, Boulevard Henri Becquerel, 14074 Caen, France

ARTICLE INFO

Article history:
Received 29 October 2014
Received in revised form
8 December 2014
Accepted 10 December 2014
Available online 11 December 2014

Keywords:
Kappa opioid receptor
JDTic
(3*R*,4*R*)-3,4-dimethyl-4-(3-hydroxyphenyl) piperidine
Selectivity
Docking

ABSTRACT

Novel *N*- and *O*-fluoroalkyl derivatives of the highly potent KOR antagonist JDTic were designed and synthesized. Their opioid receptor properties were compared in both *in vitro* binding assays and modeling approach. All compounds displayed nanomolar affinities for KOR. The fluoropropyl derivatives were more active than their fluoroethyl analogues. *N*-Fluoroalkylation was preferable to O-alkylation to keep a selective KOR binding. Compared to JDTic, the *N*-fluoropropyl derivative **2** bound to KOR with an only 4-fold lower affinity and a higher selectivity relative to MOR and DOR [$Ki_{(\kappa)}$ = 1.6 nM; $Ki_{(\mu)}/Ki_{(\kappa)}$ = 12; $Ki_{(\delta)}/Ki_{(\kappa)}$ = 159 for **2** *versus* $Ki_{(\kappa)}$ = 0.42 nM; $Ki_{(\mu)}/Ki_{(\kappa)}$ = 9; $Ki_{(\delta)}/Ki_{(\kappa)}$ = 85 for JDTic]. Modeling studies based on the crystal structure of the JDTic/KOR complex revealed that fluorine atom in ligand **2** was involved in specific KOR binding. Ligand **2** was concluded to merit further development for KOR exploration.

1. Introduction

The kappa opioid receptor (KOR, OPRK or κ) belongs to the subfamily of G-protein–coupled receptors (GPCRs) and is closely associated to the action of dynorphin (DYN) peptides as specific endogenous ligands [1]. KOR shares extensive homology with mu (MOR, OPRM or μ) and delta (DOR, OPRD or *δ*) opioid receptor subtypes, but remains unique by its pharmacology and physiological effects [2]. The three opioid receptors, KOR, MOR and DOR, regulate major functions including pain, emotional tone, appetite and reward circuitry. It is well established that KOR agonists produce an aversive effect, whereas agonists at the MOR and DOR sites are rewarding and reinforcing [3–6]. KOR is widely expressed in human throughout the central and peripheral nervous system, and is the most abundant OR in brain [7–11]. High levels of KOR mRNA have been detected in cerebral regions such as the ventral tegmental area, nucleus accumbens, prefrontal cortex, hippocampus, striatum, amygdala and hypothalamus, thought to be critical in mood modulation, motivation, stress reactivity, perception, learning memory, and behavior response to drugs. Growing evidence indicates that changes in DYN/KOR system contribute to symptom clusters that are shared by various psychiatric and addictive disorders (i.e., decreased motivation and negative affect), and that KOR disruption produces anti-stress effects [12–16]. Consequently, KOR is strongly believed to be a molecular key-target to investigate the mechanisms involved in the psychopathologies and to elaborate new therapeutic strategies. This finding has recently stimulated interest in the development of KOR antagonists as pharmacotherapies to treat depression, anxiety, schizophrenia, alcoholism, drugs seeking and relapse [17–22]. Specific KOR antagonists also represent valuable candidates as *in vivo* imaging agents to map KORs in brain and to examine their functions both in healthy and pathological conditions. Indeed, the successful development of selective radiotracers for KOR imaging by positron emission tomography (PET) would allow new investigations of

* Corresponding author. CNRS, UMR 6301 ISTCT, LDM-TEP, GIP CYCERON, Boulevard Henri Becquerel, 14074 Caen, France.
E-mail address: perrio@cyceron.fr (C. Perrio).

http://dx.doi.org/10.1016/j.ejmech.2014.12.016
0223-5234/

neuropsychiatric and addictive disorders, and help the development of novel therapeutic agents by correlating dose, *in vivo* pharmacokinetic parameters, and receptor occupancy of novel KOR-targeting drugs.

Very few pure selective KOR antagonists are reported so far (Chart 1). Classically, the reference agents were nor-BNI (norbinaltorphimine) and GNTI (5′-guanidinonaltrindole) [23,24]. Both compounds are derived from naltrexone and depend on the *N*-cyclopropylmethyl group for their antagonist properties. First discovered nor-BNI was commonly used as the standard tool in opioid pharmacology [23], and subsequently generated GNTI was found to be slightly more potent than norBNI [norBNI: $Ki_{(\kappa)}$ = 0.24 nM, $Ki_{(\mu)}/Ki_{(\kappa)}$ = 204, $Ki_{(\delta)}/Ki_{(\kappa)}$ = 170; GNTI: $Ki_{(\kappa)}$ = 0.18 nM, $Ki_{(\mu)}/Ki_{(\kappa)}$ = 125; $Ki_{(\delta)}/Ki_{(\kappa)}$ = 257] [24,25]. *In vivo*, both morphinan-derivatives were showed to display a very slow brain uptake and release, and to antagonize the actions of KOR agonists for a long time (up to several weeks) [26–29]. Recently, a new class of aminobenzyloxyarylamides has been identified as KOR antagonists with, however, a lower potency in terms of *in vitro* affinity and selectivity compared to norBNI [30]. Among them, LY2456302 [$Ki_{(\kappa)}$ = 0.8 nM, $Ki_{(\mu)}/Ki_{(\kappa)}$ = 30, $Ki_{(\delta)}/Ki_{(\kappa)}$ = 194 *versus* $Ki_{(\kappa)}$ = 0.15 nM, $Ki_{(\mu)}/Ki_{(\kappa)}$ = 216, $Ki_{(\delta)}/Ki_{(\kappa)}$ = 43 for norBNI in the same set of evaluation experiment] was found to exhibit short-acting pharmacokinetic properties *in vivo*, and to reduce ethanol self-administration in alcohol-preferring rats [31]. LY2456302 also demonstrated activity in mouse model predictive of antidepressant-like efficacy [31], and has been advanced to phase II clinical trials for the augmentation of the antidepressant therapy in treatment-resistant depression [32]. The analogue LY2795050 was lastly labelled with carbon-11 (β^+ emitter, $t_{1/2}$ = 20.4 min) and demonstrated favorable pharmacokinetic properties and binding profile in primate by PET imaging [33,34]. To date, JDTic [35–37] that belongs to the trans-(3*R*,4*R*)-3,4-dimethyl-4-(3-hydroxylphenyl)piperidine class of compounds, represents the best established pure selective KOR antagonist in *in vitro* experiments [$Ki_{(\kappa)}$ = 0.03 nM, $Ki_{(\mu)}/Ki_{(\kappa)}$ = 338, $Ki_{(\delta)}/Ki_{(\kappa)}$ = 4935 to be compared to the above cited values for norBNI and LY2456302] [31]. A recent study has reported that there was no non-opioid target from a broad panel of 43 receptors and transporters for which JDTic showed a significant affinity [38]. *In vivo*, JDTic also demonstrated highly specific KOR antagonist properties; JDTic was reported to block the KOR agonist U50488-induced antinociception in mouse, while not antagonizing mu-subtype opioid receptor (MOR) agonist-induced analgesia [37,39]. Despite having a poor brain penetration, JDTic was found to produce in mouse, rat and rhesus monkeys, long-lasting antagonistic effects [28,29], and to display a robust effectiveness in various rodent models of depression, anxiety, alcohol seeking, nicotine withdrawal and stress-induced cocaine relapse [39–42]. JDTic has been evaluated in phase I clinical trials as drug in the treatment of cocaine addiction [43]. However adverse ventricular tachycardia effects were noticed, that were unpredictable based on the absence of cardiotoxicity in the non-human primate [44].

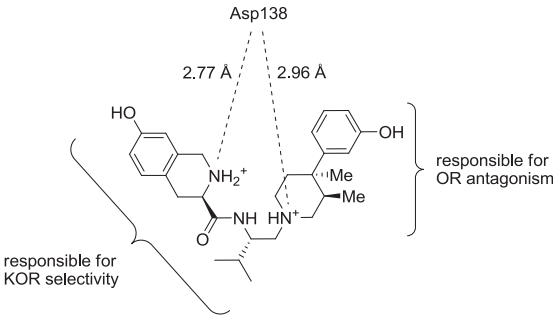

Chart 2. JDTic.

Due to its remarkable pharmacological properties, JDTic remains an important lead ligand for KOR exploration. Structural features of the receptor binding pocket were recently provided by KOR/JDTic complex co-crystallisation revealing a tight fit of JDTic in the bottom of the binding cleft forming ionic polar and extensive hydrophobic interactions with the receptor [45]. The protonated amines in both piperidine and tetrahydroisoquinoline moieties in JDTic formed salt bridges with a highly conserved aspartic acid (Asp138) side chain, probably fixing the ligand in a stabilized V-shaped conformation (Chart 2). From numerous structure–activity relationship studies conducted on JDTic, it has been well established that the (3*R*,4*R*)-3,4-dimethyl-4-(3-hydroxyphenyl)piperidine moiety provided pure opioid antagonist properties while KOR selectivity was a consequence of the N-substituent [35,36,46–51]. Only a few structural modifications on JDTic structure were allowed to retain binding properties. Introduction of a methyl group at the nitrogen atom and the hydroxyl group of the tetrahydroisoquinoline ring to give RTI-5989-97 and RTI-5989-212 respectively (Chart 1), led to minimal alteration of *in vitro* intrinsic antagonism activity [JDTic: $Ke_{(\kappa)}$ = 0.02 nM, $Ke_{(\mu)}/Ke_{(\kappa)}$ = 1255, $Ke_{(\delta)}/Ke_{(\kappa)}$ = 3830; RTI-5989-97: $Ke_{(\kappa)}$ = 0.16 nM, $Ke_{(\mu)}/Ke_{(\kappa)}$ = 1313, $Ke_{(\delta)}/Ke_{(\kappa)}$ = 3070; RTI-5989-212: $Ke_{(\kappa)}$ = 0.06 nM, $Ke_{(\mu)}/Ke_{(\kappa)}$ = 857, $Ke_{(\delta)}/Ke_{(\kappa)}$ = 1970] [36,47]. Surprisingly, the *N*-methyl derivative RTI-5989-97 was found to be a long-acting antagonist *in vivo* like JDTic, whereas the *O*-methyl analogue RTI-5989-212 displayed short duration of action [29]. In previous works, we developed the radiolabelling with carbon-11 of RTI-5989-97 (named as [^{11}C]Me-JDTic) [52]. *Ex vivo* evaluation in mouse revealed a very high specific binding of [^{11}C]MeJDTic for

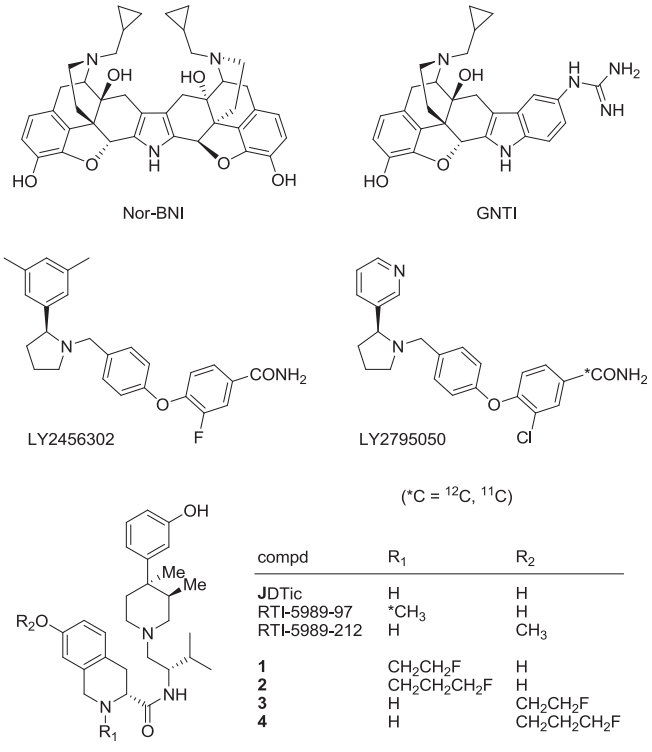

Chart 1. Structures of known potent KOR antagonists and of target compounds **1**–**4**.

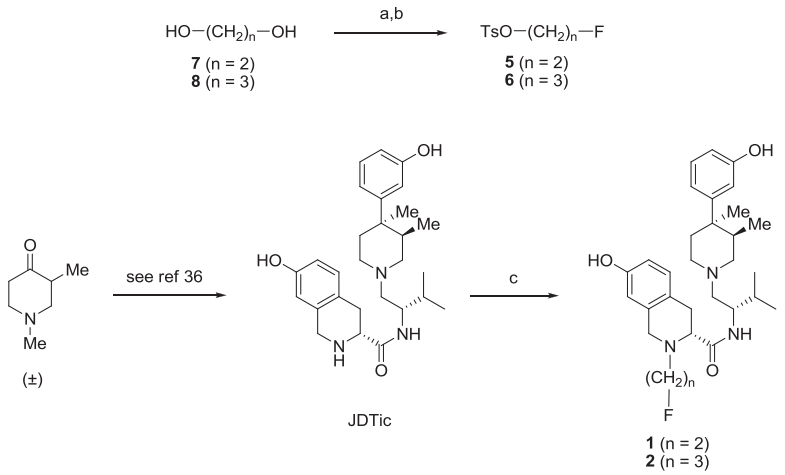

Scheme 1. Synthesis of *N*-fluoroalkyl JDTic derivatives **1** and **2**. Reagents and conditions: (a) TsCl, pyridine, 0 °C, 4–7 h; b) TBAF, ACN, reflux, 3 h; c) tosylate **5** or **6**, ACN, reflux, 72 h.

KOR but a poor brain penetration of the radioligand. Based on these promising *in vivo* results, we were next interested in further exploring *O*- and *N*-substituted JDTic derivatives in order to improve the overall *in vitro* and *in vivo* profile. We chose to derivate JDTic with lipophilic fluoroalkyl chains already known to have a beneficial impact on efficacy and selectivity in pharmaceuticals, and also to affect adsorption, distribution, metabolism, and excretion properties of the parent compound [53,54]. This approach also allowed a further radiolabeling with fluorine-18 (β^+ emitter, $t_{1/2}$ = 109.8 min) that possesses the best physical characteristics for imaging purposes, i.e., an optimal physical half-life for more convenient radiochemistry conditions and *in vivo* investigation, a high decay purity (97%), a relatively low positron energy (0.64 MeV), and relatively high experimental specific activities (correlated to the rather low abundance of fluorine in nature). Such an ^{18}F-labelled radioligand for KOR PET imaging is still missing to date. Here, we report the synthesis, pharmacological evaluation and molecular modeling studies for the *N*- and *O*-fluoroethyl and fluoropropyl JDTic analogues **1**–**4** (Chart 1). We demonstrated that both the alkylation site and the length of the alkyl chain were crucial for KOR binding and antagonism, and that fluorine atom positively participated to the ligand-receptor recognition.

2. Chemistry

N-Fluoroalkyl JDTic derivatives **1** and **2** were prepared by alkylation of JDTic with the corresponding fluoroalkyltosylates **5** and **6** as depicted in Scheme 1. JDTic was synthetized from racemic 1,3-dimethyl-4-piperidinone according to the reported method [36]. Tosylates **5** and **6** were obtained from ethylene and propylene glycols **7** and **8** according to a two-step procedure involving a bis-tosylation followed by a monofluorination reaction with TBAF [55,56].

The synthesis of *O*-fluoroalkyl JDTic derivatives **3** and **4** is displayed in Scheme 2. Compounds **3** and **4** were obtained from JDTic precursor **9** [36] and the *O*-fluoroalkyltetrahydroisoquinolinic acids **10** and **11** issued from *N*-Boc-D-7-hydroxy-1,2,3,4-tetrahydroisoquinoline-3-carboxylic acid (*N*-Boc-D-Tic) **12**. *N*-Boc-D-Tic **12** prepared as reported [57], was converted to the benzyl ester **13** by esterification with benzyl bromide. Ester **13** was subjected to an O-alkylation by reaction with the fluoroalkyltosylates **5** and **6** to yield **14** and **15** respectively. Debenzylation of **14** and **15** with KOH afforded acids **10** and **11**. Coupling of acids **10** and **12** with amine **9** using BOP followed by Boc-deprotection with TFA gave the *O*-fluoroalkyl target compounds **3** and **4**.

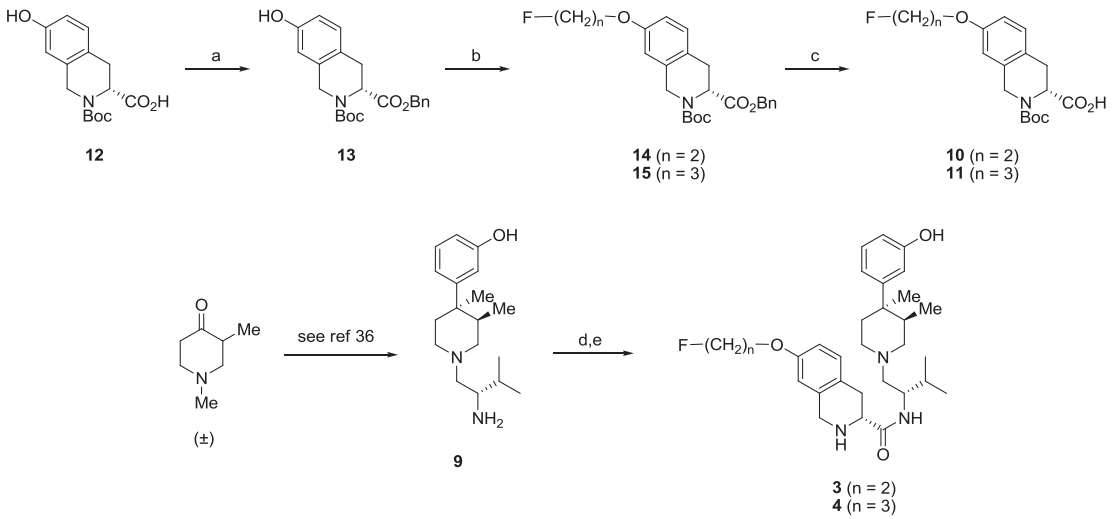

Scheme 2. Synthesis of *O*-fluoroalkyl JDTic derivatives **3** and **4**. Reagents and conditions: (a) BnBr, $NaHCO_3$, DMF, rt, 24 h; b) tosylate **5** or **6**, K_2CO_3, acetone, reflux, 48 h; c) KOH, EtOH/water, rt, 6 h; d) acid **10** or **11**, BOP, Et_3N, THF, rt, 3 h; e) TFA, DCM, −20 °C, 10 min then rt, 1 h.

Table 1
Affinity binding of references compounds, JDTic and fluoroalkyl-JDTic derivatives **1**–**4** at the different subtypes of opioid receptors (KOR, MOR and DOR).[a]

Compound	Ki (nM)[a]			Selectivity	
	KOR[b] ([3H]U69593)	MOR[c] ([3H]diprenorphine)	DOR[d] ([3H]DADLE)	MOR/KOR	DOR/KOR
U50488	0.36 ± 0.09	nd[e]	nd[e]	–	–
Naltrexone	nd[e]	0.45 ± 0.3	nd[e]	–	–
DPDPE	nd[e]	nd[e]	1.41 ± 0.30	–	–
JDTic	0.42 ± 0.10	4.00 ± 0.40	36.11 ± 5.58	9.5	85.7
N-fluoroethylJDTic **1**	5.51 ± 0.92	13.23 ± 3.39	72.81 ± 7.82	2.4	13.2
N-fluoropropylJDTic **2**	1.62 ± 0.65	19.61 ± 3.19	254.16 ± 13.42	12.2	158.9
O-fluoroethylJDTic **3**	24.01 ± 1.78	63.08 ± 5.12	81.33 ± 8.39	2.6	3.4
O-fluoropropylJDTic **4**	8.19 ± 1.77	57.52 ± 6.27	72.92 ± 7.93	7.0	8.9

[a] Data are shown as the mean values ± SD from at least three independent experiments.
[b] Rat recombinant KOR CHO cells.
[c] Human recombinant MOR HEK cells.
[d] Human recombinant DOR CHO cells.
[e] Not determined.

3. Results and discussion

3.1. OR binding studies

The four compounds **1**–**4** were each evaluated for their binding affinity for KOR, MOR and DOR. Affinities were determined by radioligand displacement experiments with specific KOR [^{3}H]U69593, MOR [^{3}H]diprenorphine and DOR [^{3}H]DADLE ligands in rat recombinant KOR CHO cells [58] and human recombinant MOR [59] or DOR [60] HEK cells. U50488, naltrexone and DPDPE were used as reference ligands of KOR, MOR and DOR respectively for validation of the binding assays. For comparison, parent JDTic prepared by our hands was also tested. The overall results were presented in Table 1, as Ki values in nM. JDTic was found to display a subnanomolar affinity (Ki = 0.42 nM) for KOR similar to the previously reported value (0.32 nM) determined in the same assay [35]. All new ligands **1**–**4** displayed KOR binding potency lower than JDTic but Ki values remained in the nanomolar range. The highest affinity and selectivity for KOR was found for the *N*-fluoropropyl derivative **2**. Affinity of **2** for KOR ($Ki_{(\kappa)}$ = 1.6 nM) was about 12-fold higher than for MOR ($Ki_{(\mu)}$ = 19.6 nM) and 158-fold higher than for DOR ($Ki_{(\delta)}$ = 254.2 nM). Compared to JDTic ($Ki_{(\kappa)}$ = 0.42 nM), compound **2** displayed an only 3.8-fold lower affinity for KOR, and a significantly higher selectivity with $Ki_{(\mu)}/Ki_{(\kappa)}$ and $Ki_{(\delta)}/Ki_{(\kappa)}$ of 12.2 and 158.9 respectively for **2** *versus* 9.5 and 85.7 for JDTic. The *N*-fluoroethyl analogue **1** ($Ki_{(\kappa)}$ = 5.5 nM) was less potent than **2**, with a 3-fold lower affinity and a very poor selectivity for KOR. The *O*-fluoroalkyl derivatives **3** ($Ki_{(\kappa)}$ = 24.0 nM) and **4** ($Ki_{(\kappa)}$ = 8.2 nM) had significantly reduced affinity and selectivity for KOR by comparison with *N*-substituted analogue **1**–**2** and JDTic. Thus, the *N*-substitution was preferred to the *O*-alkylation. Whatever the alkylation site, the longer fluoropropyl chain was better tolerated than the shorter fluoroethyl group.

Table 2
Docking results for compounds **1**–**4** compared to JDTic.

Compound	ΔG (kcal/mol)[a]	Ki (nM)[b]	Oδ1 – Np (Å)[c]	Oδ2 –Ni (Å)[d]
N-fluoroethylJDTic **1**	−10.43	22.72	2.99	3.41
N-fluoropropylJDTic **2**	−10.86	10.86	2.68	3.24
O-fluoroethylJDTic **3**	−12.19	1.16	2.74	2.85
O-fluoropropylJDTic **4**	−10.29	28.59	7.46	2.75

[a] Estimated free energy of binding ΔG.
[b] Estimated inhibition constant Ki.
[c] Distance between Asp138 Oδ1 atom and piperidine nitrogen (Np).
[d] Distance between Asp138 Oδ2 atom and isoquinoline nitrogen (Ni).

3.2. Molecular modeling

The overall pharmacological results revealed that introduction of the fluoroalkyl chain on JDTic affected its binding properties. The degree of perturbation depended on both the alkylation site and the length of the fluoroalkyl chain. Interestingly, substitution with the more sterically hindered fluoropropyl chain at the *N*-position led to a small reduced KOR affinity and an increased selectivity. Fluoroethyl substitution and *O*-alkylation provided significant loss of affinity and selectivity for KOR. In order to understand the effect of JDTic substitution, we undertook docking studies using the crystallographic structure of the KOR/JDTic complex [45]. Fluoroethyl and fluoropropyl derivatives **1**–**4** have been built and docked in the active site of the crystallographic structure of KOR showing that the affinity of the four ligands could be in part explained by the crystal structure. The docking of the four flexible compounds **1**–**4** in the binding pocket of rigid KOR has been performed using AutoDock4 [61]. For each of the four compounds **1**–**4**, the best ranked docking pose with the lower estimated free energy and the best estimated inhibition constant was chosen and analyzed.

In the crystal structure of KOR/JDTic [45], the protonated nitrogen atoms in both piperidine (Np) and isoquinoline (Ni) of JDTic form salt bridges to Asp138 side chain with bond lengths of 2.96 and 2.77 Å for Np-Oδ1 and Ni-Oδ2 respectively (Chart 2). The isoquinoline nitrogen Ni is solvent-accessible and points toward the exterior of the pocket (Fig. 1A). The hydroxyl group on isoquinoline is buried at one end of the ligand binding pocket, and participates in water-mediated interactions with residues Tyr139, Lys227 and His291 (Fig. 1B).

Construction of ligand **4** by introduction of a fluoropropyl chain on the isoquinoline hydroxyl led to a complete different location of **4** compared to JDTic (Fig. 1C). This change was due to steric hindrance in the bottom of the binding pocket. The salt bridge to Asp138 was disrupted with a very high value for the Np-Oδ1 distance (7.46 Å). Ligand **4** displayed the worst scores (ΔG = −10.29 kcal/mol; Ki = 28.59 nM; Table 2), a result in accordance with the *in vitro* pharmacological evaluation (Table 1). On the opposite, the fluoroethyl chain could be built on the hydroxyl of the isoquinoline cycle without disturbing location of JDTic structure (Fig. 1D). The Np-Oδ1 (2.74 Å) and Ni-Oδ2 (2.85 Å) distances were not significantly affected (Table 2). In addition, the docking procedure showed that the *O*-fluoroethyl JDTic **3** (ΔG = −12.19 kcal/mol; Ki = 1.16 nM) was the best ligand amongst the four compounds **1**–**4** (Table 2). This result was quite surprising on the basis of the experimental *in vitro* affinities (Table 1). In the KOR/JDTic analogues recognition, the importance

of direct or indirect interactions between isoquinoline and KOR was clearly revealed [45,51]. In a recent docking study on JDTic analogues [51], the authors suggested than removing the water-mediated interactions between KOR and ligand could result in enhanced or altered properties of the ligand. As illustration, the replacement of isoquinoline hydroxyl by hydrogen atom that prevented water-mediated interactions to take place, resulted in about a 100-fold reduction of affinity. On the other hand, when hydroxyl was replaced by a carboxamide function, the carboxamide provided a direct hydrogen-bond interaction with Lys227 without requiring an intervening water molecule, and the affinity remained unchanged. In the case of ligand **3**, the docked fluoroethyl chain took the place of the structured water molecules. The fluorine atom was found to directly interact with carboxyl oxygen of Lys227 and His291 (2.74 and 3.76 Å distances), but these interactions probably were not as favorable as hydrogen bonds. Thus, although modeling showed that ligand **3** fit well in the JDTic binding pocket, the lack of strong hydrogen bonding could explain the differences between the theoretical and experimental affinities.

A fluoroalkyl chain could also been easily built on the isoquinoline nitrogen Ni of JDTic in the binding cleft with no drastic steric clash with the KOR atoms. The Np-Oδ1 and Ni-Oδ2 distances for ligands **1** and **2** remained close to that of JDTic (Table 2). The *N*-fluoropropylJDTic **2** ($\Delta G = -10.86$ kcal/mol: Ki = 10.86 nM) was bound with a better score than the *N*-fluoroethylJDTic **1** ($\Delta G = -10.43$ kcal/mol; Ki = 22.72 nM; Table 2). This result was in agreement with the experimental *in vitro* affinities (Table 1). Ligand **1** with a shorter fluoroethyl chain was bound slightly more loosely to KOR (Fig. 1E, Table 2) than the fluoropropyl analogue **2**. This difference was due to some steric hindrance around the fluorine atom. Indeed, introduction of the fluoroethyl chain led to positioning the fluorine atom too close to KOR residues, leading to a slight shift toward a more loosely bound position. With the longer fluoropropyl substituent, the fluorine atom could nicely interact with the hydroxyl group of Tyr312 side chain with a 3.84 Å distance between fluorine and hydroxyl (Fig. 1F). This distance is higher (4.47 Å) with *N*-fluoroethyl JDTic **1** (Fig. 1E). Thus, the F–OH interaction for ligand **2** provided supplementary ligand-receptor interaction which could

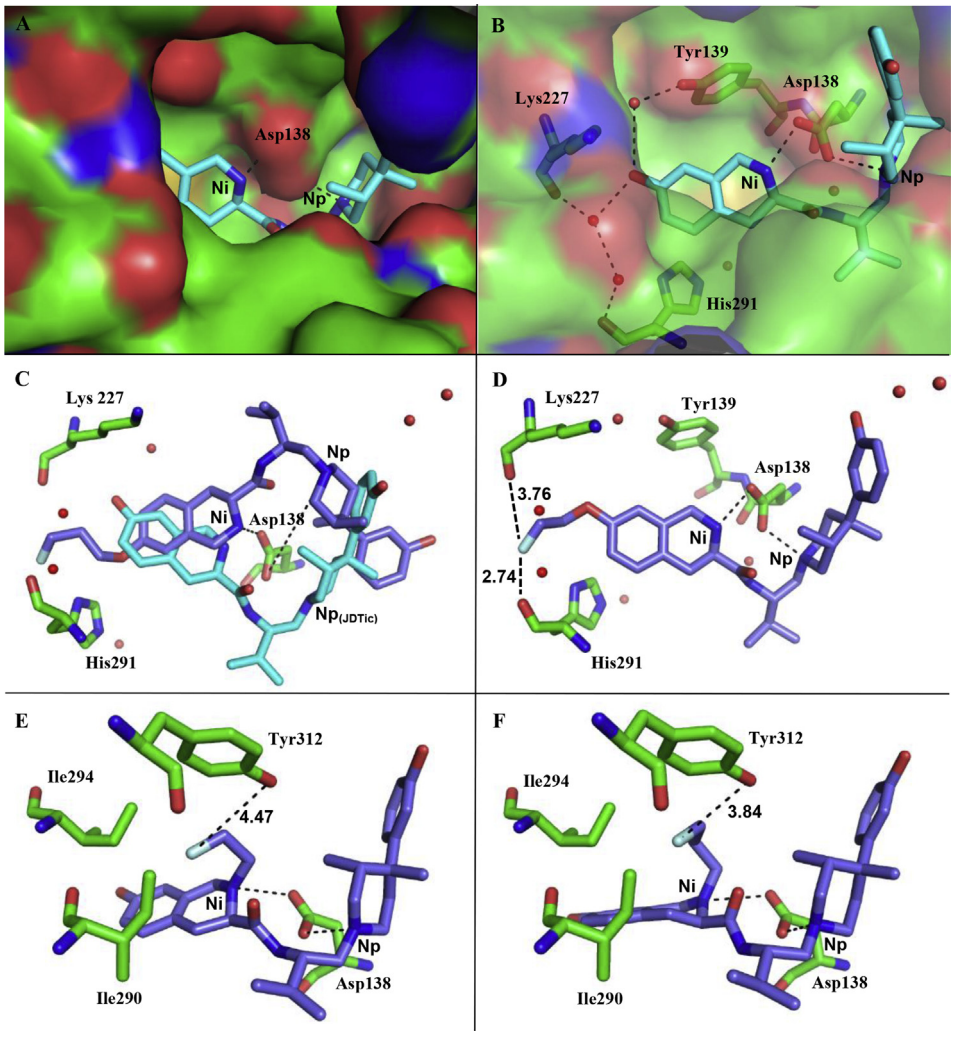

Fig. 1. Best Docking Poses of Fluoroalkyl Derivatives **1**–**4** in the Ligand KOR Binding Pocket. (A) JDTic bound in its KOR binding pocket (KOR is shown with its solvent-accessible surface). (B) Water-mediated interactions between JDTic isoquinoline hydroxyl and KOR residues (KOR is shown with its solvent-accessible surface in transparency). (C) *O*-FluoropropylJDTic **4** and JDTic for comparison. (D) *O*-FluoroethylJDTic **3** with the fluoroethyl chain taking the place of two water molecules. (E) *N*-FluoroethylJDTic **1**. (F) *O*-FluoropropylJDTic **2**. In all panels, JDTic, fluoroalkyl derivatives **1**–**4** and the selected KOR residues in interaction with the ligands are shown as capped sticks colored by atom type and with carbon atoms colored green (KOR), cyan (JDTic) and purple (derivatives **1**–**4**); the water molecules are shown as red spheres. (For interpretation of the references to colour in this figure legend, the reader is referred to the web version of this article.)

contribute to a better recognition with KOR. In addition, as Tyr312 is not conserved in the OR family (Trp in MOR and Leu in DOR) [45,62], the lack of a hydroxyl group interacting with the fluorine atom in MOR and DOR could explain the high selectivity of ligand **2** for KOR.

4. Conclusion

In summary, fluoroalkylation on tetrahydroisoquinoline ring of JDTic provided compounds with nanomolar affinity for KOR. Potency was strongly dependent on the alkylation site and the length of the fluoroalkyl chain. Alkylation of the isoquinoline nitrogen was preferred to *O*-alkylation of the isoquinoline hydroxyl. The *N*-fluoropropyl derivative **2** was only 4-fold less affine than JDTic. The fluoroethyl analogue **1** and the *O*-fluoroalkyl derivatives **3**–**4** were found to be significantly less potent. Interestingly, *N*-fluoropropyl ligand **2** displayed increased KOR selectivity relative to MOR and DOR compared to JDTic. Modeling studies highlighted the contribution of the *N*-fluoropropyl chain in the selective receptor binding by revealing interaction between fluorine atom in **2** and Tyr312 hydroxyl from KOR. Thus, the overall results provided new insights onto KOR recognition by JDTic-based compounds. Pharmacological properties of **2** suggested that this ligand may be considered as a potential candidate for radiolabelling with fluorine-18 for KOR PET imaging, and may represent a valuable tool for further KOR exploration.

5. Experimental

5.1. Chemistry

All reactions were performed under anhydrous conditions and an atmosphere of nitrogen. All reagents were purchased from Acros Organics, Fluka or Sigma–Aldrich and were used as commercially supplied. Anhydrous THF, DCM and ACN were obtained from a Mbraun SPS-800 solvents delivery system. HPLC solvents were purchased from Merck, Sigma–Aldrich or SDS. ^{1}H and ^{13}C NMR were recorded on Brucker DPX 300 at 300.0 MHz (^{1}H), 75.5 MHz (^{13}C) and 282.4 MHz (^{19}F) or on Brucker DPX 400 at 400.0 MHz (^{1}H), 100.6 MHz (^{13}C) and 376.4 MHz (^{19}F). Samples were dissolved in an appropriate deuterated solvent ($CDCl_3$, MeOD). Chemical shifts (δ) are quoted in parts per million (ppm) and referenced to proton resonances resulting from incomplete deuteration of the NMR solvent. Coupling constants (J) are given in Hz. Coupling patterns are abbreviated as follows: s (singlet), d (doublet), t (triplet), q (quadruplet), m (mutiplet), dt (doublet of triplet), qd (quadruplet of doublet). MS and high resolution mass spectra (HRMS) were recorded using a Waters Q-TOF micro spectrometer by electrospray ionisation (ESI). Relative intensities are given in brackets. Infrared spectra were recorded on a Thermo Nicolet 350 FT-IR ATR spectrometer. Only selected absorbances are reported (ν in cm^{-1}). Melting points were determined on a Barnstead Electrothermal IA 9100 Mp apparatus and are uncorrected. Optical rotations were measured with a Perkin–Elmer 341 polarimeter. Elemental analyses were performed on a ThermoQuest analyser CHNS and were within ±0.4% of the calculated values. Flash column chromatography was carried out on silica gel (Merck Kieselgel 60 F254, 40–63 μm). Analytical thin layer chromatography (TLC) was performed on Merck aluminium-backed plates pre-coated with silica (0.2 mm, 60 F254) which were visualized by quenching of ultraviolet fluorescence (λ = 254 and 366 nm) or by ninhydrin, $KMnO_4$, vanillin or phosphomolybdic acid hydrate spray reagent. High Performance Liquid Chromatography (HPLC) was carried out by a Merck L-6200 pump and a Merck L-4250 UV–visible detector.

5.1.1. *((R)-2-(2-Fluoroethyl)-7-hydroxy-N-((S)-1-((3R,4R)-4-(3-hydroxyphenyl)-3,4-dimethylpiperidin-1-yl)-3-methylbutan-2-yl)-1,2,3,4-tetrahydroisoquinoline-3-carboxamide* ***1***

A solution of JDTic (100 mg, 0.22 mmol) [36] and fluoroethyltosylate **5** (48 mg, 0.22 mmol) [55] in ACN (1 mL) was refluxed for 72 h. The solvent was removed under reduced pressure and the residue was purified by chromatography on silica gel (DCM/MeOH from 98:2 to 95:5 v/v) to give the title compound as a yellow solid (38 mg, 35%): m.p.: 116–118 °C; $[\alpha]_D^{25}$: +81.2° (*c* 0.35, EtOH); ^{1}H NMR (MeOD): δ 0.69 (d, J = 6.9 Hz, 3H), 0.86–0.93 (m, 6H), 1.28 (s, 3H), 1.51–1.56 (m, 1H), 1.81–1.88 (m, 1H), 1.95–1.98 (m, 1H), 2.16–2.24 (m, 1H), 2.28–2.45 (m, 3H), 2.50–2.63 (m, 2H), 2.69–2.73 (m, 1H), 2.83–3.08 (m, 4H), 3.50 (t, J = 6.3 Hz, 1H), 3.72 and 7.00 (AB, d, J = 14.7 Hz, 2H), 3.87–3.93 (m, 1H), 4.50–4.53 (m, 1H), 4.67–4.70 (m, 1H), 6.57–6.64 (m, 3H), 6.72–6.77 (m, 2H), 6.94 (d, J = 8.1 Hz, 1H), 7.11 (t, J = 7.8 Hz, 1H); ^{13}C NMR (MeOD): δ 16.5, 17.7, 19.8, 27.9, 29.5, 32.0, 39.2, 39.9, 51.7, 52.6, 53.4, 55.8 (d, J_{C-F} = 19.0 Hz), 56.9, 61.9, 64.2, 83.1 (d, J_{C-F} = 165.7 Hz), 113.4, 113.7, 114.1, 115.1, 117.9, 126.0, 129.8, 130.1, 137.3, 154.4, 157.1, 158.3, 173.5; IR (neat): ν 3336, 1667, 1615, 1505, 1454; MS (ESI$^+$): *m/z* 512.4 ([M+H]$^+$); HRMS (ESI$^+$) Calcd for $C_{30}H_{42}FN_3O_3$ (M$^+$): 511.3210; Found: 511.3245. Anal. Calcd. for $C_{30}H_{42}FN_3O_3 \cdot H_2O$: C, 68.03%; H, 8.37%; N, 7.93%; Found: C, 68.46%; H, 8.62%; N, 8.13%.

5.1.2. *(3R)-2-(3-Fluoropropyl)-1,2,3,4-tetrahydro-7-hydroxy-N-((S)-1-((3R,4R)-4-(3-hydroxyphenyl)-3,4-dimethylpiperidin-1-yl)-3-methylbutan-2-yl)isoquinoline-3-carboxamide* ***2***

A solution of JDTic (100 mg, 0.22 mmol) [36] and fluoropropyltosylate **6** (48 mg, 0.22 mmol) [56] in ACN (1 mL) was refluxed for 72 h. The solvent was removed under reduced pressure and the residue purified by chromatography on silica gel (DCM/MeOH from 98/2 to 95/5) to give the title compound as a yellow solid (42 mg, 37%): m.p.: 124–126 °C; $[\alpha]_D^{25}$: +87.7° (*c* 0.40, CH_3Cl); ^{1}H NMR (MeOD): δ 0.72 (d, J = 7.0 Hz, 3H), 0.88–0.94 (m, 6H), 1.29 (s, 3H), 1.59 (d, J = 13.0 Hz, 1H), 1.87–2.00 (m, 4H), 2.23 (dt, J = 4.3 and 13.0 Hz, 1H), 2.45–2.49 (m, 3H), 2.63–2.80 (m, 5H), 2.97–2.99 (m, 2H), 3.43 (t, J = 6.0 Hz, 1H), 3.59 and 3.99 (AB, d, J = 14.8 Hz, 2H), 3.90–3.93 (m, 1H), 4.47 (t, J = 5.6 Hz, 1H), 4.59 (t, J = 5.6 Hz, 1H), 6.60–6.65 (m, 3H), 6.74–6.78 (m, 2H), 6.94 (d, J = 8.1 Hz, 1H), 7.11 (t, J = 7.9 Hz, 1H); ^{13}C NMR (MeOD): δ 16.5, 17.9, 19.8, 27.9, 29.7 (d, J_{C-F} = 19.7 Hz), 30.2, 31.5, 39.2, 39.9, 49.9, 51.7, 52.7 (d, J_{C-F} = 11.2 Hz), 56.9, 61.6, 64.3, 83.2 (d, J_{C-F} = 164.0 Hz), 113.4, 113.7, 114.0, 115.1, 117.9, 125.8, 129.7, 130.2, 137.4, 152.7, 157.0, 158.3, 175.9; IR (neat): ν 3249, 1644, 1614, 1503, 1446. MS (ESI$^+$): *m/z* 526.4 ([M+H]$^+$); HRMS (ESI$^+$) Calcd for $C_{31}H_{45}FN_3O_3$ ([M+H]$^+$): 526.3445; Found: 526.3426. Anal. Calcd. for $C_{31}H_{44}FN_3O_3 \cdot H_2O$: C, 68.48%; H, 8.53%; N, 7.73%; Found: C, 68.85%; H, 8.95%; N, 7.77%.

5.1.3. *(R)-2-tert-Butyl-3-benzyl-3,4-dihydro-7-hydroxyisoquinoline-2,3(1H)-dicarboxylate* ***13***

To a solution of *N*-Boc-D-7-hydroxy-1,2,3,4-tetrahydroisoquinoline-3-carboxylic acid (*N*-Boc-D-Tic) **12** (1.90 g, 9.8 mmol) [57] and $NaHCO_3$ (940 mg, 19.6 mmol) in DMF (80 mL) was added dropwise benzyl bromide (5.80 mL, 49.2 mmol). The reaction mixture was stirred at room temperature for 24 h and ice cooled water was added. After extraction with EtOAc, the organic fraction was washed with water, dried over $MgSO_4$, filtered and concentrated under reduced pressure. The residue was purified by chromatography on silica gel (pentane/diethyl ether from 100:0 to 70:30 v/v) to give the title compound as a white solid (1.10 g, 38%): m.p.: 115–116 °C; ^{1}H NMR (MeOD) (rotamers): δ 1.39 (s, 4.5H), 1.50 (s, 4.5H), 3.02–3.19 (m, 2H), 4.38–4.57 (m, 2H), 4.83 (t, J = 5.0 Hz, 0.5H), 4.98–5.07 (m, 2.5H), 6.52–6.53 (m, 0.5H), 6.58–6.62 (m, 1.5H), 6.90–6.94 (m, 1H), 7.08–7.15 (m, 2H), 7.25–7.29 (m, 3H); ^{13}C NMR (MeOD) (rotamers): δ 28.5, 28.7, 31.7, 31.9, 45.4, 46.1, 54.9,

56.3, 67.8, 82.0, 113.6, 113.7, 115.0, 115.2, 123.8, 124.2, 128.7, 129.1, 129.2, 129.4, 129.5, 129.9, 130.4, 135.2, 135.8, 137.2, 156.8, 157.3, 157.5, 157.6, 172.9, 173.3; IR (neat): ν 2978, 1722, 1687, 1502, 1475; MS (ESI^+): *m/z* 406.2 ($[M+Na]^+$); HRMS (ESI^+) Calcd for $C_{22}H_{25}NNaO_5$ ($[M+Na]^+$): 406.1630; Found: 406.1632. Anal. Calcd. for $C_{22}H_{25}NO_5$: C, 68.91%; H, 6.57%; N, 3.65%; Found: C, 68.98%; H, 7.07%; N, 3.82%.

5.1.4. (R)-3-Benzyl-2-tert-butyl-7-(2-fluoroethoxy)-3,4-dihydroisoquinoline-2,3(1H)-dicarboxylate **14**

A solution of phenol **13** (300 mg, 0.78 mmol), fluoroethyltosylate **5** (205 mg, 0.94 mmol) [55] and K_2CO_3 (204 mg, 1.48 mmol) in acetone (6 mL) was refluxed for 48 h. The solution was cooled to room temperature and a saturated aqueous solution of NH_4Cl was added. After extraction with EtOAc, the organic fraction was dried over $MgSO_4$, filtered and concentrated under reduced pressure. The residue was purified by chromatography on silica gel (hexane/diethyl ether from 100:0 to 60:40) to give the title compound as a white solid (260 mg, 78%): m.p.: 64–65 °C; ^1H NMR ($CDCl_3$) (rotamers): δ 1.40 (s, 4.5H), 1.51 (s, 4.5H), 3.05–3.26 (m, 2H), 4.11–4.14 (m, 1H), 4.21–4.23 (m, 1H), 4.47 (AB, d, J = 16.5 Hz, 1H), 4.61–4.68 (m, 2H), 4.80–4.83 (m, 1.5H), 4.98–5.09 (m, 2H), 5.18 (m, 0.5H), 6.66 (m, 1H), 6.74 (m, 1H), 7.02 (d, J = 8.4 Hz, 1H), 7.14 (m, 2H), 7.27–7.30 (m, 3H); ^{13}C NMR ($CDCl_3$) (rotamers): δ 28.3, 28.4, 30.6, 31.0, 44.4, 44.9, 52.9, 54.6, 66.7, 67.2 (d, J_{C-F} = 20.3 Hz), 80.8, 81.8 (d, J_{C-F} = 180.5 Hz), 111.8, 112.1, 113.7, 124.6, 124.7, 127.7, 128.0, 128.2, 128.4, 128.5, 129.0, 129.6, 130.0, 134.1, 135.1, 135.5, 135.7, 154.8, 155.4, 157.4, 171.4, 171.8; IR (neat): ν 2978, 1722, 1687, 1502, 1475; MS (ESI^+) *m/z* 452.2 ($[M+Na]^+$); HRMS (ESI^+) Calcd for $C_{24}H_{28}FNNaO_5$ ($[M+Na]^+$): 452.1849; Found: 452.1837.

5.1.5. (R)-3-Benzyl-2-tert-butyl-7-(3-fluoropropoxy)-3,4-dihydroisoquinoline-2,3(1H)-dicarboxylate **15**

A solution of phenol **13** (250 mg, 0.65 mmol), fluoropropyltosylate **6** (180 mg, 0.77 mmol) [56] and K_2CO_3 (172 mg, 1.24 mmol) in acetone (5 mL) was refluxed for 48 h, cooled to room temperature and a saturated aqueous solution of NH_4Cl was added. After extraction with EtOAc, the organic fraction was dried over $MgSO_4$, filtered and concentrated under reduced pressure. The residue was purified by chromatography on silica gel (hexane/diethyl ether from 100:0 to 70:30) to give the title compound as a white solid (245 mg, 85%); m.p.: 70–73 °C; $[\alpha]_D^{25}$: +6.5° (*c* 1.13, $CHCl_3$); ^1H NMR ($CDCl_3$) (rotamers): δ 1.40 (s, 4.5H), 1.51 (s, 4.5H), 2.14 (m, 2H), 3.04–3.24 (m, 2H), 4.06 (t, J = 6.0 Hz, 3H), 4.48 and 4.62 (AB, d, J = 16.2 Hz, 2H), 4.65 (dt, J = 41.3 and 6.0 Hz, 2H), 4.82 (t, J = 5.1 Hz, 0.5H), 4.99–5.09 (m, 2H), 5.19 (m, 0.5H), 6.62–6.74 (m, 2H), 7.00 (d, J = 8.4 Hz, 1H), 7.14 (m, 2H), 7.28 (m, 4H); ^{13}C NMR ($CDCl_3$) (rotamers): δ 28.3, 28.4, 30.3, 30.6 (d, J_{C-F} = 20.3 Hz), 44.4, 44.9, 52.9, 54.6, 63.5 (d, J_{C-F} = 4.8 Hz), 66.7, 80.6, 80.7 (d, J_{C-F} = 163.4 Hz), 111.6, 112.1, 113.4, 113.5, 124.1, 124.3, 127.7, 127.9, 128.0, 128.2, 128.4, 128.5, 128.9, 129.5, 134.0, 135.1, 135.6, 135.7, 154.8, 155.5, 157.6, 157.7, 171.4, 171.8; IR (neat): ν 2978, 1723, 1689, 1585, 1502; MS (ESI^+) *m/z* 466.2 ($[M+Na]^+$); Anal. Calcd. for $C_{25}H_{30}FNO_5$: C, 67.70%; H, 6.82%; N, 3.16%; Found: C, 67.97%; H, 7.16%; N, 3.39%.

5.1.6. (R)-2-(tert-Butoxycarbonyl)-7-(2-fluoroethoxy)-1,2,3,4-tetrahydroisoquinoline-3-carboxylic acid **10**

To a solution of benzyl ester **14** (250 mg, 0.58 mmol) in EtOH (5 mL) was added dropwise a solution of KOH (134 mg, 2.39 mmol) in water (5 mL). The reaction mixture was vigorously stirred at room temperature for 6 h, and EtOH was removed under reduced pressure. The aqueous solution was acidified to pH 6 with dilute HCl. After extraction with DCM, the organic fraction was washed with water, dried over $MgSO_4$, and concentrated under reduced pressure. The residue was purified by chromatography on silica gel (hexane/diethyl ether from 100:0 to 0:100) to give the title compound as a white solid (110 mg, 60%): m.p.: 60–62 °C; $[\alpha]_D^{25}$: −4.2° (*c* 1.00, $CHCl_3$); ^1H NMR ($CDCl_3$) (rotamers): δ 1.41–1.51 (m, 9H), 3.03–3.22 (m, 2H), 4.11–4.14 (m, 1H), 4.21–4.23 (m, 1H), 4.43 (d, J = 16.8 Hz, 1H), 4.60–4.67 (m, 2H), 4.75–4.82 (m, 1.5H), 5.09 (m, 0.5H), 6.66–6.77 (m, 2H), 7.06 (d, J = 8.2 Hz, 1H); ^{13}C NMR ($CDCl_3$) (rotamers): δ 28.2, 28.4, 30.1, 30.6, 44.1, 44.7, 52.5, 54.3, 67.1 (d, J_{C-F} = 20.4 Hz), 81.0, 81.9 (d, J_{C-F} = 169.9 Hz), 111.9, 112.1, 113.7, 124.4, 124.5, 128.9, 129.6, 133.9, 135.0, 154.8, 155.7, 157.3, 157.4, 177.1, 177.8; IR (neat): ν 2976, 1695, 1615, 1504, 1475; MS (ESI^-): *m/z* 338.1 ($[M-H]^-$).

5.1.7. (R)-2-(tert-Butoxycarbonyl)-7-(3-fluoropropoxy)-1,2,3,4-tetrahydroisoquinoline-3-carboxylic acid **11**

To a solution of benzyl ester **15** (220 mg, 0.50 mmol) in EtOH (5 mL) was added dropwise a solution of KOH (114 mg, 2.03 mmol) in water (5 mL). The solution was vigorously stirred for 6 h at room temperature, and EtOH was removed under reduced pressure. The aqueous solution was acidified to pH 6 with dilute HCl. After extraction with DCM, the organic fraction was washed with water, dried over $MgSO_4$, and concentrated under reduced pressure. The residue was purified by chromatography on silica gel (hexane/diethyl ether from 100:0 to 60:40) to give the title compound as a white solid (120 mg, 70%): m.p. 70–73 °C; $[\alpha]_D^{25}$: −13.1° (*c* 0.82, $CHCl_3$); ^1H NMR ($CDCl_3$) (rotamers): δ 1.41 (s, 4.5H), 1.50 (s, 4.5H), 2.14 (qd, J = 26.1 and 6.0, 2H), 3.02–3.21 (m, 2H), 4.05 (t, J = 6.0 Hz, 2H), 4.39–4.47 (m, 1H), 4.62–4.75 (m, 3.5H), 5.07–5.09 (m, 0.5H), 6.64–6.75 (m, 2H), 7.04 (d, J = 8.1 Hz, 1H); ^{13}C NMR ($CDCl_3$) (rotamers): δ 28.2, 28.4, 30.1, 30.3 (d, J_{C-F} = 11.0 Hz), 44.1, 44.8, 63.5, 63.6, 68.4, 80.7 (d, J_{C-F} = 163.4 Hz), 80.9, 111.7, 112.0, 113.6, 124.1, 128.9, 129.5, 134.9, 154.8, 157.7, 177.2; IR (neat): ν 2974, 1695, 1615, 1504, 1475; MS (ESI^-): *m/z* 352.1 ($[M-H]^-$).

5.1.8. (3R)-7-(2-Fluoroethoxy)-1,2,3,4-tetrahydro-N-((S)-1-((3R,4R)-4-(3-hydroxyphenyl)-3,4-dimethylpiperidin-1-yl)-3-methylbutan-2-yl)isoquinoline-3-carboxamide **3**

To a solution of carboxylic acid **10** (110 mg, 0.32 mmol), amine **9** (94 mg, 0.32 mmol) [36] and Et_3N (151 μL, 1.12 mmol) in THF (20 mL) was added BOP (166 mg, 0.37 mmol). The mixture was stirred at room temperature for 3 h and diluted in diethyl ether. The solution was washed with a saturated aqueous solution of $NaHCO_3$ and water, dried over $MgSO_4$, filtered and concentrated under reduced pressure. The residue was purified by chromatography on silica gel (DCM/MeOH from 100:0 to 80:20). The residue was dissolved in DCM (2 mL) and TFA (0.75 mL) was added dropwise at −20 °C. The reaction mixture was stirred at −20 °C for 10 min, and then at room temperature for 1 h. The mixture was washed with a saturated aqueous solution of $NaHCO_3$ and water, dried over $MgSO_4$, filtered and concentrated under reduced pressure. The residue was purified by chromatography on silica gel (DCM/MeOH from 100:0 to 80:20) to give the title compound as a yellow solid (11 mg, 6%); m.p. 113–116 °C; $[\alpha]_D^{25}$: +79.2° (*c* 0.25, EtOH); ^1H NMR ($CDCl_3$): δ 0.77 (d, J = 7.1 Hz, 3H), 0.95–0.99 (m, 6H), 1.34 (s, 3H), 1.59–1.71 (m, 2H), 1.86–1.93 (m, 1H), 2.06–2.16 (m, 1H), 2.32–2.39 (m, 1H), 2.76–3.07 (m, 7H), 3.65–3.69 (m, 2H), 4.02–4.07 (m, 4H), 4.52–4.55 (m, 1H), 4.63–4.66 (m, 1H), 6.59–6.77 (m, 5H), 7.04–7.11 (m, 2H); ^{13}C NMR ($CDCl_3$): δ 17.9, 19.2, 30.3, 30.9, 38.2, 38.5, 55.9, 56.8, 59.2, 67.1, 80.8, 111.7, 112.8, 113.4, 117.2, 126.9, 129.2, 130.3, 156.7, 175.0; IR (neat): ν 3341, 1677, 1618, 1503, 1433; MS (ESI^+): *m/z* 512.4 ($[M+H]^+$); HRMS (ESI^+) Calcd for $C_{30}H_{43}FN_3O_3$ ($[M+H]^+$): 512.3288; Found: 512.3281; Anal. Calcd. for $C_{30}H_{42}FN_3O_3 \cdot H_2O$: C, 68.03%; H, 8.37%; N, 7.93%; Found: C, 68.41%; H, 8.58%; N, 8.26%.

*5.1.9. (3R)-7-(3-Fluoropropoxy)-1,2,3,4-tetrahydro-N-((S)-1-((3R,4R)-4-(3-hydroxyphenyl)-3,4-dimethylpiperidin-1-yl)-3-methylbutan-2-yl)isoquinoline-3-carboxamide **4***

To a solution of carboxylic acid **11** (120 mg, 0.34 mmol), amine **9** (100 mg, 0.34 mmol) [36] and Et_3N (161 μL, 1.16 mmol) in THF (20 mL) was added BOP (176 mg, 0.39 mmol). The mixture was stirred at room temperature for 3 h and diluted with diethyl ether. The mixture was washed with a saturated aqueous solution of $NaHCO_3$ and water, dried over $MgSO_4$, filtered and concentrated under reduced pressure. The residue was purified by chromatography on silica gel (DCM/MeOH from 100:0 to 80:20). The residue was dissolved in DCM (2 mL) and TFA (0.75 mL) was added dropwise at −20 °C. The reaction mixture was stirred at −20 °C for 10 min, and then at room temperature for 1 h. The mixture was washed with a saturated aqueous solution of $NaHCO_3$ and water, dried over $MgSO_4$, filtered and concentrated under reduced pressure. The residue was purified by chromatography on silica gel (DCM/MeOH from 100:0 to 80:20) to give the title compound as a yellow solid (12 mg, 7%): m.p. 105–107 °C; $[\alpha]_D^{25}$: +82.7° (*c* 0.25, EtOH); ^1H NMR ($CDCl_3$): δ 0.75–0.80 (m, 3H), 0.94–1.08 (m, 6H), 1.33 (s, 3H), 1.43–1.47 (m, 1H), 1.61–2.10 (m, 5H), 2.28–2.46 (m, 2H), 2.59–3.16 (m, 6H), 3.58–3.78 (m, 3H), 4.01–4.20 (m, 4H), 4.61–4.62 (m, 1H), 4.73–4.74 (m, 1H), 6.58–6.60 (m, 1H), 6.66–6.77 (m, 4H), 7.04–7.13 (m, 2H); ^{13}C NMR ($CDCl_3$): δ 16.1, 16.6, 17.9, 19.9, 27.9, 28.8, 31.4, 32.3, 39.2, 39.8, 46.1, 46.7, 51.5, 52.1, 56.3, 61.2, 64.8, 64.9, 80.6, 113.0, 113.5, 114.7, 117.9, 126.3, 130.1, 136.2, 151.9, 157.2, 158.4, 159.3, 174.5; IR (neat): ν 3339, 1675, 1618, 1510, 1431. MS (ESI^+) *m/z* 526.4 ($[M+H]^+$); HRMS (ESI^+) Calcd for $C_{31}H_{45}FN_3O_3$ ($[M+H]^+$): 526.3445; Found: 526.3437. Anal. Calcd. for $C_{31}H_{44}FN_3O_3 \cdot H_2O$: C, 68.48%; H, 8.53%; N, 7.73%; Found: C, 68.88%; H, 8.97%; N, 7.98%.

5.2. OR binding assays

Binding affinities for KOR, MOR and DOR were determined by radioligand displacement experiments with specific KOR [^3H] U69593 (1 nM), MOR [^3H]diprenorphine (0.4 nM) and DOR [^3H] DADLE (0.5 nM) ligands in rat recombinant KOR CHO cells [58] and human recombinant MOR [59] or DOR [60] HEK cells according to published procedures. Non-specific binding was defined as the binding of radioligand in the presence of naltrexone (10 μM for KOR and DOR, 1 μM for MOR). Assays were first validated with U50488, naltrexone and DPDPE used as reference ligands of KOR, MOR and DOR respectively. Eight different concentrations of each compounds **1**–**4**, JDTic and reference ligands were tested. All assays were conducted in 50 mM Tris buffer (pH 7.4) at room temperature for 60 min for KOR binding and for 120 min for MOR and DOR binding. All experiments were performed in triplicate.

5.3. Docking studies

The molecular modeling studies were performed using the published crystal structure of KOR in complex with JDTic (Protein Data Bank code 4DJH) [45]. *Discovery Studio 3.5* suite (Accelrys, San Diego, CA, USA) was used to add hydrogen atoms and to build the fluoroalkyl compounds **1**–**4** on the JDTic structure. An automatic docking procedure has been performed for each of the four fluoroalkyl compounds, with *AutoDock4* [61], using a flexible ligand, a rigid receptor and a Lamarckian genetic algorithm with the default setting parameters. For each compound, the best scoring ligand with the lower estimated free energy and the best estimated inhibition constant was chosen. Fig. 1 was prepared using *PYMOL* (DeLano Scientific, CA, USA).

Acknowledgments

This research was supported by the "Région Basse-Normandie" ("IMADEP" project 12P03303) and the European Regional Development Fund (ERDF, ISCE-Chem & INTERREG Iva program 4061 grant). The authors thank the CRIHAN (Centre de Ressources Informatiques de Haute Normandie), the European Community (FEDER) for the molecular modeling software Discovery Studio (Accelrys, San Diego, CA, USA) and Jana Sopkova-de Oliveira Santos (CERMN, Caen, France) for her help in building compounds with Discovery Studio.

Appendix A. Supplementary data

Supplementary data related to this article can be found at http://dx.doi.org/10.1016/j.ejmech.2014.12.016.

References

[1] B.N. Dhawan, F. Cesselin, R. Raghubir, T. Reisine, P.B. Bradley, P.S. Porthoghese, M. Hamon, Pharmacol. Rev. 48 (1996) 567–592.
[2] M. Minami, M. Satoh, Neurosci. Res. 23 (1995) 121–145.
[3] M. Waldhoer, S.E. Bartlett, J.L. Whistler, Annu. Rev. Biochem. 73 (2004) 953–990.
[4] J.M. van Ree, M.A. Gerrits, L.J. Vanderschuren, Pharmacol. Rev. 51 (1999) 341–396.
[5] P.E. Lutz, B.L. Kieffer, Trends Neurosci. 36 (2013) 195–206.
[6] J. Le Merrer, J.A.J. Becker, K. Befort, B.L. Kieffer, Physiol. Rev. 89 (2009) 1379–1412.
[7] J.M. Hiller, L.Q. Fan, Neurochem. Res. 21 (1996) 1333–1345.
[8] D. Peckys, G.B. Landwehrmeyer, Neuroscience 88 (1999) 1093–1135.
[9] F. Simonin, C. Gaveriaux-Ruff, K. Befort, H. Matthes, B. Lannes, G. Micheletti, M.G. Mattéi, G. Charron, B. Bloch, B. Kieffer, Proc. Natl. Acad. Sci. U. S. A. 92 (1995) 7006–7010.
[10] J. Peng, S. Sarkar, L. Chang, Drug Alcohol Depend. 124 (2012) 223–228.
[11] A.M. Mathieu-Kia, L.Q. Fan, M.J. Kreek, E.J. Simon, J.M. Hiller, Brain Res. 893 (2001) 121–134.
[12] H.A. Tejeda, T.S. Shippenberg, R. Henriksson, Cell Mol. Life Sci. 69 (2012) 857–896.
[13] A. Van't Veer, W.A. Carlezon, Psychopharmacology 229 (2013) 435–452.
[14] Y. Shirayama, H. Ishida, M. Iwata, G.I. Hazama, R. Kawahara, R.S.J. Duman, J. Neurochem. 90 (2004) 1258–1268.
[15] B.B. Land, M.R. Bruchas, J.C. Lemos, M. Xu, E.J. Melief, C.J. Chavkin, Neuroscience 28 (2008) 407–414.
[16] R. Przewłocki, B. Przewłocka, Eur. J. Pharmacol. 429 (2001) 79–91.
[17] A.T. Knoll, E.G. Meloni, J.B. Thomas, F.I. Caroll, W.A. Carlezon Jr., J. Pharmacol. Exp. Ther. 323 (2007) 838–845.
[18] J.V. Aldrich, J.P. McLaughlin, AAPS J. 11 (2009) 312–322.
[19] W.A. Carlezon, C. Béguin, A.T. Knoll, B.M. Cohen, Pharmacol. Ther. 123 (2009) 334–343.
[20] B.M. Walker, G.F. Koob, Neuropsychopharmacology 33 (2008) 643–652.
[21] F.I. Carroll, W.A. Carlezon Jr., J. Med. Chem. 56 (2013) 2178–2195.
[22] M. Urbano, M. Guerrero, H. Rosen, E. Roberts, Bioorg. Med. Chem. Lett. 24 (2014) 2021–2032.
[23] P.S. Portoghese, A.W. Lipkowski, A.E. Takemorif, J. Med. Chem. 30 (1987) 238–239.
[24] W.C. Stevens, R.M. Jones Jr., G. Subramanian, T.G. Metzger, D.M. Ferguson, P.S. Portoghese, J. Med. Chem. 43 (2000) 2759–2769.
[25] R.M. Jones, P.S. Portoghese, Eur. J. Pharmacol. 396 (2000) 49–52.
[26] H. Zhang, Y.-G. Shi, J.H. Woods, S.J. Watson, M.-C. Ko, Eur. J. Pharmacol. 570 (2007) 89–96.
[27] S. Kishioka, N. Kiguchi, Y. Kobayashi, C. Yamamoto, F. Saika, N. Wakida, M.-C. Ko, J.H. Woods, Neurosci. Lett. 552 (2013) 98–102.
[28] T.A. Munro, L.M. Berry, A. Van't Veer, C. Béguin, F.I. Carroll, Z. Zhao, W.A. Carlezon Jr., B.M. Cohen, BMC Pharmacol. 12 (2012) 5.
[29] E.J. Melief, M. Miyatake, F.I. Carroll, C. Béguin, W.A. Carlezon Jr., B.M. Cohen, S. Grimwood, C.H. Mitch, L. Rorick-Kehn, C. Chavkin, Mol. Pharmacol. 80 (2011) 920–929.
[30] C.H. Mitch, S.J. Quimby, N. Diaz, C. Pedregal, M.G. de la Torre, A. Jimenez, Q. Shi, E.J. Canada, S.D. Kahl, M.A. Statnick, D.L. McKinzie, D.R. Benesh, K.S. Rash, V.N. Barth, J. Med. Chem. 54 (2011) 8000–8012.
[31] L.M. Rorick-Kehn, J.M. Witkin, M.A. Statnick, E.L. Eberle, J.H. McKinzie, S.D. Kahl, B.M. Forster, C.J. Wong, X. Li, R.S. Crile, D.B. Shaw, A.E. Sahr, B.L. Adams, S.J. Quimby, N. Diaz, A. Jimenez, C. Pedregal, C.H. Mitch, K.L. Knopp, W.H. Anderson, J.W. Cramer, D.L. McKinzie, Neuropharmacology 77 (2014) 131–144.
[32] http://clinicaltrials.gov/ct2/show/NCT01913535.
[33] M.-Q. Zheng, N. Nabulsi, S.J. Kim, G. Tomasi, S.-F. Lin, C. Mitch, S. Quimby, V. Barth, K. Rash, J. Masters, A. Navarro, E. Seest, E.D. Morris, R.E. Carson,

Y. Huang, J. Nucl. Med. 54 (2013) 455–463.
[34] S.J. Kim, M.-Q. Zheng, N. Nabulsi, D. Labaree, J. Ropchan, S. Najafzadeh, R.E. Carson, Y. Huang, E.D. Morris, J. Nucl. Med. 54 (2013) 1668–1674.
[35] J.B. Thomas, R.N. Atkinson, R.B. Rothman, S.E. Fix, S.W. Mascarella, N.A. Vinson, H. Xu, C.M. Dersch, Y. Lu, B.E. Cantrell, D.M. Zimmerman, F.I. Carroll, J. Med. Chem. 44 (2001) 2687–2690.
[36] J.B. Thomas, R.N. Atkinson, N.A. Vinson, J.L. Catanzaro, C.L. Perretta, S.E. Fix, S.W. Mascarella, R.B. Rothman, H. Xu, C.M. Dersch, B.E. Cantrell, D.M. Zimmerman, F.I. Carroll, J. Med. Chem. 46 (2003), 3127–3131-37.
[37] I. Carroll, J.B. Thomas, L.A. Dykstra, A.L. Granger, R.M. Allen, J.L. Howard, G.T. Pollard, M.D. Aceto, L.S. Harris, Eur. J. Pharmacol. 501 (2004) 111–119.
[38] T.A. Munro, X.-P. Huang, C. Inglese, M.G. Perrone, A. Van't Veer, F.I. Carroll, C. Béguin, W.A. Carlezon Jr., N.A. Colabufo, B.M. Cohen, B.L. Roth, PLoS One 8 (2013) e70701.
[39] P.M. Beardsley, J.L. Howard, K.L. Shelton, F.I. Carroll, Psychopharmacology 183 (2005) 118–126.
[40] J.R. Schank, A.L. Goldstein, K.E. Rowe1, C.E. King, J.A. Marusich, J.L. Wiley, F.I. Carroll, A. Thorsell, M. Heilig, Addict. Biol. 17 (2012) 634–647.
[41] F.I. Carroll, L.S. Harris, M.D. Aceto, Eur. J. Pharmacol. 524 (2005) 89–94.
[42] K.J. Jackson, F.I. Carroll, S.S. Negus, M.I. Damaj, Psychopharmacology 210 (2010) 285–294.
[43] http://clinicaltrials.gov/ct2/results?term=JDTic.
[44] http://www.mclean.harvard.edu/kappa-therapeutics-2013/pdf/Kappa-Therapeutics-2013-Complete-Program.pdf.
[45] H. Wu, D. Wacker, M. Mileni, V. Katritch, G.W. Han, E. Vardy, W. Liu, A.A. Thompson, X.-P. Huang, F.I. Carroll, S.W. Mascarella, R.B. Westkaemper, P.D. Mosier, B.L. Roth, V. Cherezov, R.C. Stevens, Nature 485 (2012) 327–332.
[46] D.M. Zimmerman, R. Nickander, J.S. Horng, D.T. Wong, Nature 275 (1978) 332–334.
[47] J.P. Cueva, T.B. Cai, W.S. Mascarella, J.B. Thomas, H.A. Navarro, F.I. Carroll, J. Med. Chem. 52 (2009) 7463–7472.
[48] J.B. Thomas, S.E. Fix, R.B. Rothman, S.W. Mascarella, C.M. Dersch, B.E. Cantrell, D.M. Zimmerman, F.I. Carroll, J. Med. Chem. 47 (2004) 1070–1073.
[49] S.P. Runyon, L.E. Brieaddy, S.W. Mascarella, J.B. Thomas, H.A. Navarro, J.L. Howard, G.T. Pollard, F.I. Carroll, J. Med. Chem. 53 (2010) 5290–5301.
[50] T.B. Cai, Z. Zou, J.B. Thomas, L. Brieaddy, H.A. Navarro, F.I. Carroll, J. Med. Chem. 51 (2008) 1849–1860.
[51] C.M. Kormos, M.G. Gichinga, R. Maitra, S.P. Runyon, J.B. Thomas, L.E. Brieaddy, S.W. Mascarella, H.A. Navarro, F.I. Carroll, J. Med. Chem. 57 (2014) 7367–7381.
[52] G. Poisnel, F. Oueslati, M. Dhilly, J. Delamare, C. Perrio, D. Debruyne, L. Barré, Nucl. Med. Biol. 35 (2008) 561–569.
[53] S. Purser, P.R. Moore, S. Swallow, V. Gouverneur, Chem. Soc. Rev. 37 (2008) 320–330.
[54] K. Müller, C. Faeh, F. Diederich, Science 317 (2007) 1881–1886.
[55] Y.Z. Ponce, S. Mavel, T. Assaad, S.E. Kruse, S.M. Parsons, P. Emond, S. Chalon, N. Giboureau, M. Kassiou, D. Guilloteau, Bioorg. Med. Chem. 13 (2005) 745–753.
[56] T.W. Bell, H.-J. Choi, W. Harte, M.G.B. Drew, J. Am. Chem. Soc. 125 (2003) 12196–12210.
[57] C. Liu, J.B. Thomas, L. Brieaddy, B. Berrang, F.I. Carroll, Synthesis 6 (2008) 856–858.
[58] F. Meng, G.-X. Xie, R.C. Thompson, R.C. Thompson, A. Mansour, A. Goldstein, S.J. Watson, H. Akil, Proc. Natl. Acad. Sci. U. S. A. 90 (1993) 9954–9958.
[59] S. Zhang, Y. Tong, M. Tian, R.N. Dehaven, L. Cortesburgos, E. Mansson, F. Simonin, B. Kieffer, L. Yu, J. Pharmacol. Exp. Ther. 286 (1998) 136–141.
[60] F. Simonin, K. Befort, C. Gavériaux-Ruff, H. Matthes, V. Nappey, B. Lannes, G. Micheletti, B. Kieffer, Mol. Pharmacol. 46 (1994) 1015–1021.
[61] G.M. Moris, R. Huey, W. Lindstrom, M.F. Sanner, R.K. Belew, D.S. Goodsell, A.J. Olson, J. Comput. Chem. 16 (2009) 2785–2791.
[62] K. Martinez-Mayorga, K.G. Byler, A.B. Yongye, M.A. Giulianotti, C.T. Dooley, R.A. Houghten, Eur. J. Med. Chem. 66 (2013) 114–121.